



Enriching the isotopic toolbox for migratory connectivity analysis: a new approach for migratory species breeding in remote or unexplored areas

Sasha Pekarsky^{1*}, Alon Angert², Barbara Haese³, Martin Werner³, Keith A. Hobson⁴ and Ran Nathan¹

¹Movement Ecology Lab, Dept. of Ecology, Evolution & Behavior, Alexander Silberman Institute of Life Sciences, The Hebrew University of Jerusalem, Jerusalem 91904, Israel, ²The Institute of Earth Sciences, The Hebrew University of Jerusalem, Jerusalem 91904, Israel, ³Alfred Wegener Institute for Polar and Marine Research (AWI), Bussestr. 24, Bremerhaven 27570, Germany, ⁴Environment Canada, 11 Innovation Blvd, Saskatoon, SK, Canada S7N 3H5

ABSTRACT

Aim We examined three potential enhancements of the stable isotope technique for elucidating migratory connectivity in birds inhabiting poorly studied areas, illustrated for Eurasian cranes (*Grus grus*) that overwinter in and migrate through Israel. First, we examined the use of oxygen stable isotopes ($\delta^{18}\text{O}$), seldom applied for this purpose. Second, we examined the relationship between ambient water $\delta^{18}\text{O}$ and hydrogen stable isotope ($\delta^2\text{H}$) values derived from various models, to determine the geographical origins of migrants. Third, we introduced the use of probabilistic distribution modelling to refine the assignment to origin of migrants lacking detailed distribution maps.

Location Feather samples were collected in the Hula Valley (northern Israel) and across the species breeding range in north Eurasia.

Methods We analysed $\delta^{18}\text{O}$ and $\delta^2\text{H}$ in primary and secondary flight feathers using standard mass spectrometry. The maximum entropy (MAXENT) model was used to map the probability surface of potential breeding areas, as a Bayesian prior for assigning Hula Valley cranes to potential breeding grounds.

Results We found that $\delta^{18}\text{O}$ was suitable and informative. The soil water isoscape performed better for $\delta^{18}\text{O}$ while precipitation isoscape was preferable for $\delta^2\text{H}$. The MAXENT-based probability surface largely refined assignments. Overall, most (>85%) cranes were assigned to the area west of the Ural Mountains, but for two individuals, most of the assigned area (>90%) was farther east, suggesting, for the first time, that Eurasian cranes may undertake the North Asia–Middle East (and perhaps Africa) migration flyway.

Main conclusions Our results call for broader use of $\delta^{18}\text{O}$ in migratory connectivity studies and for application of probabilistic distribution modelling. We also encourage investigation of factors determining $\delta^{18}\text{O}$ and $\delta^2\text{H}$ integration into animal tissues. The proposed framework may help improve our understanding of migratory connectivity of species inhabiting previously unexplored areas and thus contribute to the development of efficient conservation plans.

Keywords

Atmosphere GCM, deuterium, ECHAM5, *Grus grus*, isoscape, isotopic assignment to origin, MAXENT, migratory connectivity, oxygen-18, stable isotopes.

*Correspondence: Sasha Pekarsky, Movement Ecology Lab, Dept. of Ecology, Evolution & Behavior, Alexander Silberman Institute of Life Sciences, The Hebrew University of Jerusalem, Jerusalem 91904, Israel.
E-mail: alexandr.pekarsky@mail.huji.ac.il

INTRODUCTION

Migratory organisms are greatly influenced by events occurring during different stages of their annual cycle, which may take place at vastly distant geographical areas (Webster &

Marra, 2005). Identifying linkages between breeding and non-breeding stages is essential for understanding population ecology and dynamics, life-history strategies, evolution of migration patterns and mechanisms of genetic differentiation (Boulet & Norris, 2006; Rolshausen *et al.*, 2009). Moreover,

designing effective conservation plans depends on understanding ecological processes operating over the entire range of a threatened species, since protection on the breeding grounds, for example, would be insufficient if conservation measures are inadequate at overwintering sites (Martin *et al.*, 2007). Furthermore, management of individuals in overwintering hotspots requires identifying the source (breeding) populations to assess migration/staging strategies and the risks of population or even species extinction, if epidemics or other local catastrophes strike at this hotspot.

Recent technological developments have delineated migratory connectivity using both extrinsic (e.g. satellite biotelemetry) and intrinsic (e.g. stable isotopes and genetic markers) methods (Webster *et al.*, 2002). The primary advantage of intrinsic markers is that initial marking of individuals is unnecessary and every capture becomes a 'recapture' (Hobson, 2005). Particularly, measurements of stable isotope ratios of naturally occurring elements in animal tissues were shown to effectively establish migratory connections in a wide range of taxa (Rubenstein & Hobson, 2004; Hobson & Wassenaar, 2008). More specifically, measurements of stable hydrogen isotopes ($\delta^2\text{H}$) in bird feathers are effective since they strongly correlate with the amount-weighted mean $\delta^2\text{H}$ values in precipitation water ($\delta^2\text{H}_p$) that vary systematically at global scales (Hobson, 2011). However, $\delta^2\text{H}$ measurements of complex organic materials are complicated since keratinous materials undergo uncontrolled hydrogen isotopic exchange with the ambient atmospheric vapour (Wassenaar & Hobson, 2003; Meier-Augenstein *et al.*, 2013). Despite the tight relationship observed in meteoric water between $\delta^2\text{H}$ and stable oxygen isotopes ($\delta^{18}\text{O}$) (Craig, 1961; Dansgaard, 1964), and no exchangeable oxygen in keratinous materials, the relationship between $\delta^{18}\text{O}$ values in feathers ($\delta^{18}\text{O}_f$) and $\delta^{18}\text{O}$ values in precipitation ($\delta^{18}\text{O}_p$) has thus far been explored only in one study (Hobson *et al.*, 2004).

The main concern with using $\delta^{18}\text{O}$ in animal forensics (Hobson *et al.*, 2004) is its lower naturally occurring range compared to $\delta^2\text{H}$ (e.g. *c.* 17.2‰ and *c.* 126‰, respectively, in Europe), and atmospheric oxygen being an additional oxygen source incorporated into animal tissues, whereas food and drinking water are the only sources of tissue hydrogen. Furthermore, to date, no international standards for $\delta^{18}\text{O}$ measurements in complex organics have been developed (Qi *et al.*, 2011). However, the analytical error for intrasample variation for $\delta^2\text{H}$ analysis ($\pm 3\%$ for samples and $\pm 2\%$ for keratin standards; Wassenaar & Hobson, 2006) is much higher than the intrasample variation reported for oxygen measurements ($\pm 0.4\%$; Hobson *et al.*, 2004; and $\pm 0.45\%$ in the current work, but see Qi *et al.*, 2011), implying a similar sensitivity of these isotopes in resolving geospatial origins. Moreover, larger mammals derive proportionally more of their oxygen from drinking water (Bryant & Froelich, 1995). Applying the same principle for birds, $\delta^{18}\text{O}_f$ values in large birds are expected to be linked more strongly to the isotopic values of ambient water. Therefore, using $\delta^{18}\text{O}$

measurements for studying migratory connectivity merits further examination, particularly in large birds.

For assigning geographical origins to migratory birds, likelihood-based statistics are used to propagate different sources of variance to the probability surface of origin (Wunder, 2010), and information regarding species breeding extent and distribution is used as a Bayesian prior to assignment of migrants (Hobson, 2011). Yet, breeding distribution maps remain unavailable or incomplete for many bird species, highlighting the need to develop a general analytical approach for estimating sufficiently detailed distribution maps for a wide variety of species, especially those of conservation concern.

Predicting the origin of migrants using isotopic techniques requires a rescaling equation linking feather isotopic values to those in ambient water (Wunder, 2010). This raises another important, yet neglected, limitation of current methodology: the regression–interpolation model-based isotope maps (isoscapes) are sensitive to the spatial distribution of isotope measurement stations, making such isoscapes less precise in predicting $\delta^2\text{H}_p$ and $\delta^{18}\text{O}_p$ values in areas where stations are scarce such as vast areas in northern Asia (Bowen & Revenaugh, 2003). The recently released global precipitation isoscape employing a regionalized cluster-based water isotope prediction (RCWIP) approach, significantly improved predictive accuracy and precision over classical global-fixed regression–interpolation-based models, yet was also reported to be affected by the number of stations in each region (Terzer *et al.*, 2013). The (Atmospheric) General Circulation Models (GCM), enhanced with a module for explicit simulation of water stable isotopes within the model's hydrological cycle (e.g. Jouzel *et al.*, 1987; Hoffmann *et al.*, 1998; Werner *et al.*, 2011), are capable of simulating a global distribution of $\delta^{18}\text{O}$ and $\delta^2\text{H}$ in environmental waters and thus provide isotope values in regions where precipitation measurement stations are unavailable. In this study, we used simulated values of $\delta^{18}\text{O}_p$ and $\delta^{18}\text{O}$ of soil water ($\delta^{18}\text{O}_s$) of the coupled atmosphere–land surface model ECHAM5-JSBACH-wiso (Haese *et al.*, 2013). The application of $\delta^{18}\text{O}_s$ data may better represent the water reservoir available at the base of the food chain. To the best of our knowledge, this study is the first to apply GCM-based isoscapes for animal forensics.

The breeding extent of the Eurasian crane (*Grus grus*) spans throughout North Eurasia, including vast areas in north Asia (Johnsgard, 1983) where only few isotopic measurement stations are available. Moreover, while its breeding extent is known and occurrence data are available from observations and previous studies, detailed distribution maps are lacking. Over the last two decades, the Hula Valley in northern Israel became a globally important Eurasian crane wintering and stopover site. The drastic increase in the wintering crane population in a relatively small area has resulted in a conflict with local farmers and an ecological threat of overcrowding, thus endangering >10% of the world population (Shanni *et al.*, 2011). Although Israel is considered to lie

at the eastern migration route of the species, funnelling cranes breeding in east Europe and western Russia (Shirihai, 1996), little is known about the origins of the cranes migrating through and wintering in the Hula Valley.

We aimed to implement and evaluate several novel approaches in applying stable isotopes to improve estimates of connectivity between breeding and non-breeding populations in species inhabiting poorly studied areas. As proof of concept, we used the $\delta^{18}\text{O}$ isotopic composition of cranes migrating through and wintering in the Hula Valley, to depict the probable breeding areas contributing to this globally important wintering and stopover site. More specifically, we set the following objectives: (1) To test the ability of $\delta^{18}\text{O}$ measurements as a tracer to reveal migratory connections and compare it to results derived from the more traditionally used $\delta^2\text{H}$ measurements; (2) To examine the relationship between ambient water $\delta^{18}\text{O}$ and $\delta^2\text{H}$ values derived from various models, across Europe and the Asian part of Russia, a region that has not yet been studied using stable isotopes; (3) To test the application of the GCM model $\delta^{18}\text{O}_s$ output for animal forensics; (4) To examine the efficiency of probabilistic distribution maps generated by Species Distribution Model as a Bayesian prior for assignment to origin.

METHODS

Feather sampling

A calibration set of samples from known locations was obtained from researchers, ringers and rangers throughout the species' breeding range to establish species-specific rescaling equation linking $\delta^{18}\text{O}_f$ and $\delta^2\text{H}_f$ with that of ambient water (see Table S1 in Supporting Information). Feathers were collected only in proximity to active nests. Cranes from unknown origin were sampled during the non-breeding period in the Agmon wetland and surrounding cultivated lands (5 km²) in the Hula Valley, northern Israel (35°43' E, 33°03' N), between October and April 2010–2011 and 2011–2012 (Table S2), using feathers collected from up to 1-week-old carcasses found in the study area.

We used only primary and secondary flight feathers based on, well-studied (Johnsgard, 1983; Kashentseva, 2003) moult patterns of the cranes: the post-breeding moult, during which all flight feathers are dropped and the birds remain flightless, occurs during a period of 5–6 weeks between May and August. This moulting pattern ensures that the new feathers are fully developed before fall migration, but moulting does not occur every year. We assumed cranes return to the same (or close to the same) breeding areas every year, since site fidelity is well documented for many migratory birds and Eurasian cranes in particular (Johnsgard, 1983).

Stable isotope analysis

For $\delta^{18}\text{O}$ analysis, sample cleaning and preparation was performed using standard methods (Appendix S1). The $\delta^{18}\text{O}$

measurements were performed on CO derived from high-temperature pyrolysis (1400 °C) using Sercon HT-EA (Sercon Ltd.). Helium was used as the carrier gas (80 mL min⁻¹). The HT-EA was interfaced in continuous flow mode, through a 0.5 m 5-Å molecular sieve GC column, to an isotope ratio mass spectrometer (Sercon 20–20). The GC was used to chromatographically separate N₂ from CO, and its temperature was maintained at 70 °C. Under these conditions, no tailing of N₂ into the CO peak was observed. All measurements were performed against the IAEA-601 ($\delta^{18}\text{O} = 23.14\text{‰}$) and IAEA-602 ($\delta^{18}\text{O} = 71.4\text{‰}$) benzoic acid standards.

The $\delta^2\text{H}$ measurements were performed at the Stable Isotope Hydrology and Ecology Laboratory of Environment Canada in Saskatoon, Canada, using the comparative equilibration method (Wassenaar & Hobson, 2003) through use of calibrated keratin $\delta^2\text{H}$ reference materials. $\delta^2\text{H}$ measurements were performed on H₂ derived from high-temperature (1350 °C) flash pyrolysis of 350 ± 10 µg feather subsamples using continuous-flow isotope-ratio mass spectrometry. Measurement of three keratin laboratory reference materials (CBS: -197‰, SPK: -121.6‰, and KHS: -54.1‰; corrected for linear instrumental drift) were used to calibrate unknowns.

All the isotopic values are expressed in standard delta notation, in units per mil (‰), and normalized on the VSMOW-VSLAP standard scale. For $\delta^{18}\text{O}_f$ measurements, replicate analyses of a single feather in different runs over 7 months, representing expected intrasample isotopic heterogeneity and analytical error, yielded standard deviation of 0.45‰ ($n = 6$). For every feather, we also sequentially measured two vane sample replicates, with a mean standard deviation of 0.15 ± 0.14‰ (mean ± SD, $n = 103$). For $\delta^2\text{H}_f$ measurements, analytical error was assumed to be ±2‰ based on replicate ($n = 5$) within-run measurements of keratin standards.

Water isoscapes

Data on ambient water oxygen and hydrogen isotope composition were obtained from three different methods. We used the annual amount-weighted mean since its isotopic composition is similar to the groundwater, which is the dominant water source for many wetland types inhabited by the cranes (St Amour *et al.*, 2005). First, we used $\delta^{18}\text{O}_p$ and $\delta^2\text{H}_p$ values estimated by two regression–interpolation-based models: a widely used global-fixed regression–interpolation-based (GFRI) model at 0.33° resolution (Bowen & Revenaugh, 2003, <http://www.waterisotopes.org>) and a recently introduced regionalized cluster-based water isotope prediction (RCWIP) model at 0.16° resolution (Terzer *et al.*, 2013, <http://www-naweb.iaea.org>). Second, we used the annual mean output of the coupled atmosphere–land surface model ECHAM5-JSBACH-wiso [described in detail by Haese *et al.* (2013)], which incorporates stable water isotopes as tracers in the hydrological cycle, to predict precipitation and soil

water $\delta^{18}\text{O}$ and $\delta^2\text{H}$. The model was run under present-day conditions for an average period of 30 years, average cell size of 1.8° and 31 vertical model levels (T63L31). We used the set-up assuming no isotopic fractionation during evapotranspiration as this model set-up resulted in good agreement with observational data from different GNIP stations (Haese *et al.*, 2013). A multiple regression was performed between the isotope values and the longitude and latitude at 100 randomly selected points throughout the cranes' breeding range, to assess the global patterns in the model outputs.

Prediction of potential breeding areas

To generate the probability surface of crane breeding areas, occurrence data for breeding cranes in Europe and Asia were obtained from two main sources: (1) sampling locations of feather collections, including locations not used for creating the rescaling equation; (2) breeding locations described in the literature (Table S3; unspecified geographical coordinates were extracted based on area description and figures). The records were geographically unbalanced, with Finland and Germany contributing >40% of all records, creating clumps of up to 10 records per 100 km^2 grid. As spatial filtering for reducing clumping of records improved the quality of model prediction (Kramer-Schadt *et al.*, 2013), we randomly selected records to produce not more than one sample per 100 km^2 to match the mean record clumping of other regions, reducing the total number of records to 52 (Table S4).

We used three habitat variables (topography, freshwater proximity and land cover). The topography feature was obtained from the global relief model at 60-arc second resolution (Amante & Eakins, 2009; <http://www.ngdc.noaa.gov/mgg/global/global.html>). For the freshwater proximity variable, we used the Global Lakes and Wetlands Database (GLWD) (Lehner & Döll, 2004; <http://worldwildlife.org/pages/global-lakes-and-wetlands-database>). Since cranes are known to nest in proximity to a variety of freshwater bodies (Johnsgard, 1983), we used the Euclidean Distance tool in the Spatial Analyst extension of ARCGIS (ESRI, Redlands, CA, USA) to establish a 10-km-radius buffer zone around the water bodies. For land cover classification, we used the Global Land Cover 2000 at 30-arc second resolution (GLC2000; <http://bioval.jrc.ec.europa.eu/products/glc2000/glc2000.php>; Table S5). For climate conditions, 19 WorldClim variables at 30-arc second resolution were obtained (Hijmans *et al.*, 2005; <http://www.worldclim.org>; Table S6). To reduce multicollinearity, we calculated Pearson's correlation (r) between each variable pair for 1000 random points from throughout the geographical range. We selected six variables (Table 1) with $r > 0.75$ (Dormann *et al.*, 2013), keeping variables with the highest permutation importance.

We used maximum entropy modelling (MAXENT version 3.3.3k; Phillips *et al.*, 2006) to generate the probability surface. All grids were subject to equal area projection (Europe_Albers_Equal_Area_Conic) to avoid latitudinal variation in cell area (Elith *et al.*, 2006) and resampled at a

Table 1 Climatic variables used in model building

Variable	Description
BIO1	Annual Mean Temperature
BIO2	Mean Diurnal Range [Mean of monthly (max temp – min temp)]
BIO8	Mean Temperature of Wettest Quarter
BIO17	Precipitation of Driest Quarter
BIO18	Precipitation of Warmest Quarter
BIO19	Precipitation of Coldest Quarter

uniform 1-km spatial resolution. The regularization multiplier was set to the default value of one. All variables were defined as continuous, except for freshwater proximity and land cover which were defined as categorical.

The predictive power of the MAXENT-derived maps was evaluated using cross-validation. The occurrence dataset was randomly partitioned into two groups, using 75% for training and the remaining 25% for validation. To create the potential breeding area probability surface, we used the mean probabilities of 10 replicates, each based on all 52 records. Model performance was evaluated using AUC, a threshold-independent measure representing the probability that a presence site will be ranked above a random background site (by default 10,000 random background 'pseudo-absence' points are sampled). AUC ranges between 1 (perfect match) and 0.5 (random). Models with $\text{AUC} > 0.75$ are considered potentially useful (Elith *et al.*, 2006).

Identifying crane origins

To assign birds to geographical origins, we created a probability surface of origin for cranes sampled in the Hula Valley during the wintering and migration seasons, by combining (1) the expected $\delta^{18}\text{O}_f$ and $\delta^2\text{H}_f$ values, based on the relationship between measured values of $\delta^{18}\text{O}_f$ and $\delta^2\text{H}_f$ collected in the breeding sites and $\delta^{18}\text{O}$ and $\delta^2\text{H}$ in the ambient water in these sites, with (2) the predicted probability surface of crane breeding areas. Both data layers were reclassified using the Spatial Analyst extension of ARCGIS, to encompass only the known breeding range from the literature (Johnsgard, 1983); hence, it was assumed to provide the most updated approximation of the realized breeding niche of the cranes. All isoscapes were resampled to have cell size of 1.8° . The layers were imported into MATLAB R2013b (The Mathworks Inc., Natick, MA, USA) for assignment calculations.

Since the rescaling equation parameters are uncertain, we assumed that $\delta^{18}\text{O}_f$ and $\delta^2\text{H}_f$ at any geographical location are better characterized as a distribution of potential values rather than a single one. To model the observed variance estimates for each collection site, we normally distributed the residuals of the regression of $\delta^{18}\text{O}_f$ and $\delta^2\text{H}_f$ with the predicted value within the rescaled isoscapes. The likelihood that each cell within the rescaled feather isoscape represents a potential origin for each sampled crane was estimated using

$$f(y|\mu, \sigma) = \left(\frac{1}{\sqrt{2\pi\sigma^2}} \right) \exp \left[-\frac{1}{2\sigma^2} (y - \mu)^2 \right], \quad (1)$$

where $f(y|\mu, \sigma)$ is the probability that any given cell on the isoscape represents a potential origin for an individual with $\delta^{18}\text{O}_f$ and $\delta^2\text{H}_f$ values y , given an expected mean (μ) of $\delta^{18}\text{O}_f$ and $\delta^2\text{H}_f$ based on the predicted value within the rescaled isoscape and the expected standard deviation (σ). The σ value was estimated using the standard deviation of the residuals from the regression equation. We used the standard deviation of the residuals because it accounts for the deviation of the $\delta^{18}\text{O}_f$ and $\delta^2\text{H}_f$ from the expected geographical pattern which is present in the ambient water, thus representing the variance in the predicted value within the calibrated isoscape. This procedure resulted in a surface of spatially explicit probability densities for each individual bird (i.e. one surface per bird).

We incorporated the probability surface of potential breeding areas by applying Bayes' rule to compute the probability of location (a given cell) being the origin, using

$$f_x = \frac{f(y|\mu, \sigma)f_b}{\sum_i f(y|\mu, \sigma)f_b} \quad (2)$$

where f_x is the normalized posterior probability of origin for each individual, $f(y|\mu, \sigma)$ is estimated from Eqn. 1, and f_b represents the spatially explicit prior probabilities of the loca-

tion being an origin of each individual. Afterwards, we summed results for all the Hula Valley samples. The resulting grid was normalized by dividing by the total number of individuals, for creating posterior probability surface of origin for the population.

RESULTS

We collected primary flight feathers from 102 individuals during the non-breeding season in the Hula Valley (Table S2). The isotopic analysis of the samples showed no significant relationship between $\delta^{18}\text{O}_f$ and $\delta^2\text{H}_f$ ($r^2 = -0.07$, $P = 0.393$, $n = 0.103$). Isotopic analysis of 15 samples collected at the breeding sites was performed to quantify the relationship between $\delta^{18}\text{O}_f$ and $\delta^2\text{H}_f$ and the ambient water estimates in the collection sites (Table S1). Stepwise multiple regression showed that the longitude of the collection site had a stronger contribution to both $\delta^{18}\text{O}_f$ and $\delta^2\text{H}_f$ ($\beta = 0.83$, $P < 0.001$ and, respectively, $\beta = 0.76$, $P < 0.001$), while the latitude had a weaker contribution to $\delta^2\text{H}_f$ ($\beta = 0.42$, $P < 0.05$) and no contribution to $\delta^{18}\text{O}_f$ ($\beta = 0.19$, $P = 0.23$). Both longitude and latitude significantly contributed to the $\delta^{18}\text{O}_p$ and $\delta^2\text{H}_p$ values produced by all three models (Fig. 1a–c, Table 2). In the GCM-based $\delta^{18}\text{O}_s$ and $\delta^2\text{H}_s$ values, however, the longitude had a strong contribu-

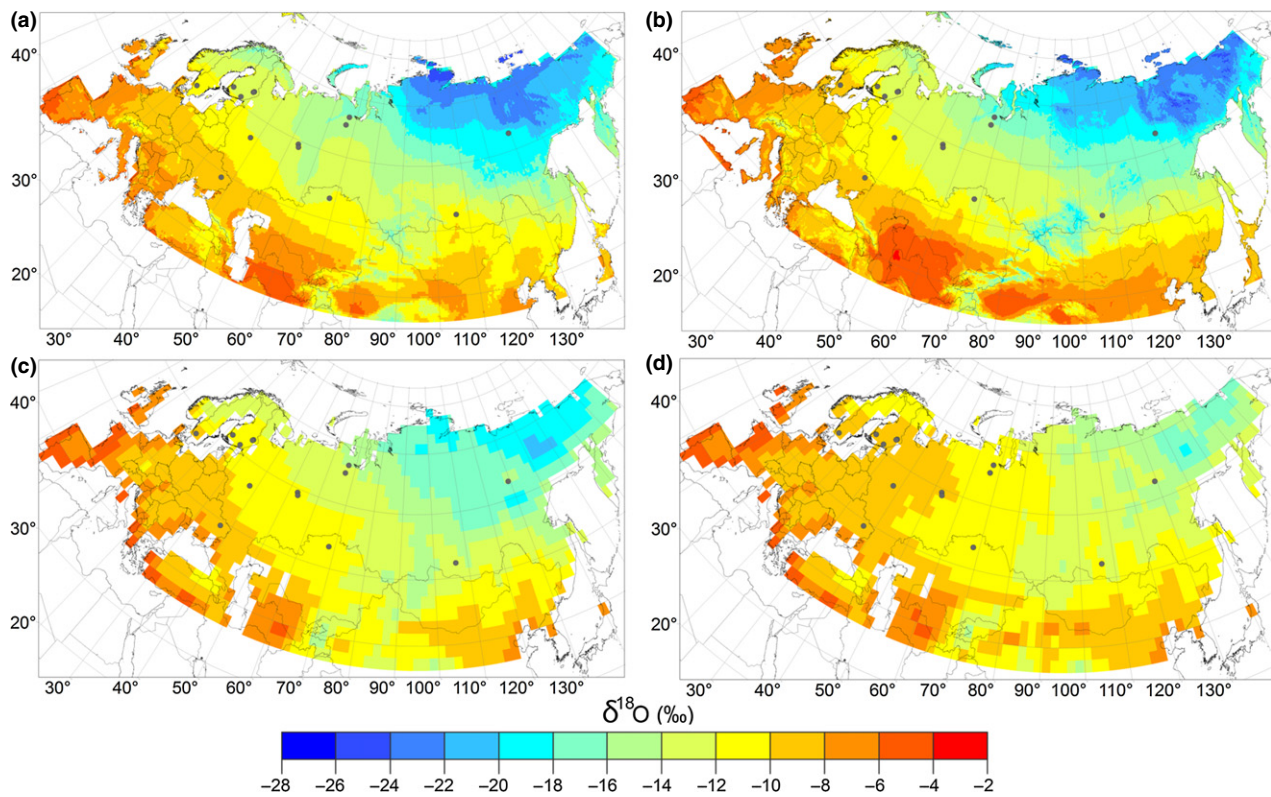


Figure 1 Estimated isoscapes of ambient water $\delta^{18}\text{O}$ and locations of the collection sites (shown on the map as black circles) of feathers used to estimate the calibration equations. (a) Global-fixed regression–interpolation-based precipitation $\delta^{18}\text{O}$ isoscape (Bowen & Revenaugh, 2003), (b) regionalized cluster-based precipitation isoscape (Terzer *et al.*, 2013), (c) GCM-based precipitation $\delta^{18}\text{O}$ and (d) GCM-based soil water $\delta^{18}\text{O}$ isoscapes (Haese *et al.*, 2013). The cell size of the isoscapes was 0.33, 0.16, 0.18 and 0.18 degrees, respectively. Projection: Albers.

Table 2 Stepwise multiple regression analysis of ambient water $\delta^{18}\text{O}$ and $\delta^2\text{H}$ with the longitude and latitude, at 100 random points throughout the known breeding range of the cranes. GFRI-p, global-fixed regression–interpolation-based precipitation (Bowen & Revenaugh, 2003); RCWIP-p, regionalized cluster-based precipitation isoscape (Terzer *et al.*, 2013); GCM-p and GCM-s, GCM-based precipitation and GCM-based soil water (Haese *et al.*, 2013)

Model	Variable	Unstandardized coefficients		Standardized coefficients		<i>t</i> value	<i>P</i> value
		Coefficient	Std. Error	Beta			
GFRI-p	$\delta^{18}\text{O}$	Lon	−0.061	0.003	−0.790	−20.744	<0.001
		Lat	−0.283	0.019	−0.561	−14.724	<0.001
	$\delta^2\text{H}$	Lon	−0.509	0.021	−0.790	−23.886	<0.001
		Lat	−2.497	0.139	−0.594	−17.945	<0.001
RCWIP-p	$\delta^{18}\text{O}$	Lon	−0.060	0.003	−0.806	−19.640	<0.001
		Lat	−0.249	0.020	−0.514	−12.521	<0.001
	$\delta^2\text{H}$	Lon	−0.507	0.023	−0.833	−21.622	<0.001
		Lat	−1.932	0.153	−0.486	−12.624	<0.001
GCM-p	$\delta^{18}\text{O}$	Lon	−0.056	0.003	−0.868	−21.907	<0.001
		Lat	−0.169	0.017	−0.399	−10.064	<0.001
	$\delta^2\text{H}$	Lon	−0.451	0.020	−0.865	−22.299	<0.001
		Lat	−1.406	0.132	−0.414	−10.658	<0.001
GCM-p	$\delta^{18}\text{O}$	Lon	−0.047	0.002	−0.910	−20.807	<0.001
		Lat	−0.025	0.015	−0.073	−1.679	0.097
	$\delta^2\text{H}$	Lon	−0.372	0.018	−0.906	−20.343	<0.001
		Lat	−0.234	0.119	−0.087	−1.959	0.053

Table 3 Linear regression of feather $\delta^{18}\text{O}$ and $\delta^2\text{H}$ with the ambient water $\delta^{18}\text{O}$ and $\delta^2\text{H}$ of the collection site ($n = 15$). GFRI-p, global-fixed regression–interpolation-based precipitation (Bowen & Revenaugh, 2003); RCWIP-p, regionalized cluster-based precipitation isoscape (Terzer *et al.*, 2013); GCM-p and GCM-s, GCM-based precipitation and GCM-based soil water (Haese *et al.*, 2013). * $P < 0.05$; ** $P < 0.001$

Model		Slope	Intercept	R^2
GFRI-p	$\delta^{18}\text{O}$	0.65*	18.41	0.44
	$\delta^2\text{H}$	0.74*	−30.63	0.48
RCWIP-p	$\delta^{18}\text{O}$	0.80*	20.25	0.61
	$\delta^2\text{H}$	0.98**	−7.96	0.73
GCM-p	$\delta^{18}\text{O}$	1.02*	21.95	0.59
	$\delta^2\text{H}$	1.31**	8.82	0.72
GCM-s	$\delta^{18}\text{O}$	1.51**	25.02	0.79
	$\delta^2\text{H}$	1.45*	−0.31	0.52

tion and no latitudinal significant contribution (Fig. 1d, Table 2).

The strongest correlation was found between known-origin crane $\delta^{18}\text{O}_f$ values and GCM-based $\delta^{18}\text{O}_s$ ($\delta^{18}\text{O}_{\text{GCM-s}}$), while the $\delta^2\text{H}_f$ values showed the strongest correlation with RCWIP-based $\delta^2\text{H}_p$ ($\delta^2\text{H}_{\text{RCWIP-p}}$) values (Table 3, Fig 2). Both $\delta^{18}\text{O}_f$ and $\delta^2\text{H}_f$ exhibited the weakest correlation with the GFRI-based precipitation ratios (Table 3, Fig 2). Thus, we chose the $\delta^{18}\text{O}_{\text{GCM-s}}$ and $\delta^2\text{H}_{\text{RCWIP-p}}$ isoscapes to create the rescaled feather isoscapes for $\delta^{18}\text{O}_f$ and $\delta^2\text{H}_f$ respectively. The residuals were normally distributed (Shapiro–Wilk test: $W = 0.943$, $P = 0.42$ and $W = 0.948$, $P = 0.5$ for $\delta^{18}\text{O}_{\text{GCM-s}}$ and $\delta^2\text{H}_{\text{RCWIP-p}}$, respectively) and homoscedastic for both rescaling equations.

Probabilistic distribution modelling

Prediction of potential breeding areas was performed with parameters derived using all 52 presence records and achieved a mean AUC of 0.905. The AUC of the training data was 0.908 and the test AUC was 0.873, indicating that our model performed well. The most suitable areas for cranes were predicted in western Russia, southern Scandinavia and low elevation areas in Siberia (Fig. 3).

Assignment of individual cranes to breeding location

Assignment was made based on the feather isoscape created using the rescaling equations linking $\delta^{18}\text{O}_f$ and $\delta^2\text{H}_f$ with that of the ambient water. Applying the probability surface of crane potential breeding areas (Fig. 3) as a prior for the assignment of individuals to the isoscape reduced the geographical extent of the assigned origins. To test the increase in assignment precision, we reclassified the probability maps for each individual into likely versus unlikely origins, by specifying an odds ratio of 2 : 1. The mean (\pm SD) proportion of area assigned for each individual (i.e. the number of pixels divided by the total pixel number of the breeding range) based only on the isoscape values was reduced by 17% for $\delta^{18}\text{O}$ (0.17 ± 0.08 and 0.14 ± 0.06 , respectively; Wilcoxon signed-ranks test: $Z = -8.8$, $P < 0.001$, one tailed) and 22% for $\delta^2\text{H}$ (0.29 ± 0.09 and 0.22 ± 0.07 , respectively; Wilcoxon signed-ranks test: $Z = -8.8$, $P < 0.001$, one tailed), when the prior probabilities were applied.

Comparison between the assignments performed based on $\delta^{18}\text{O}_f$ and $\delta^2\text{H}_f$ rescaled isoscapes showed that for 50% of individuals there was more than 20% congruence between

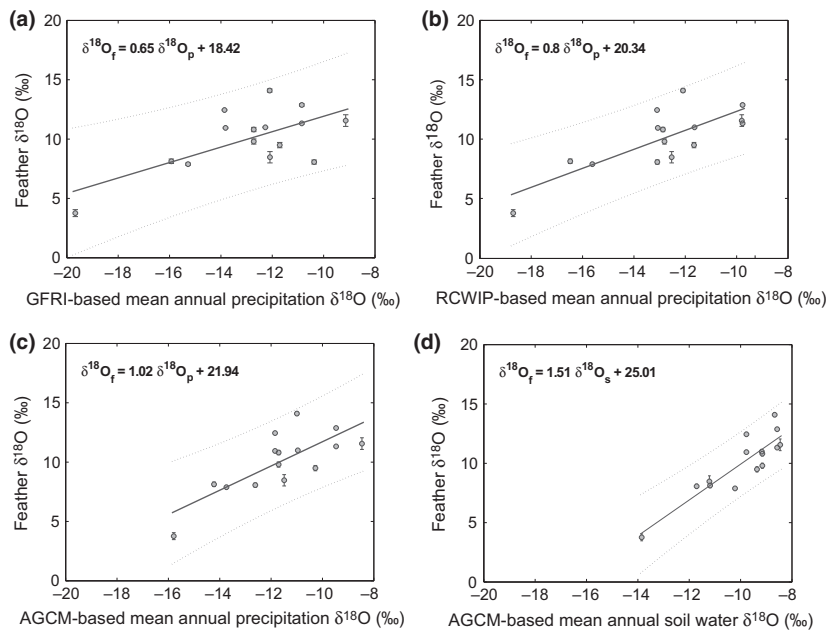


Figure 2 Regression between known Eurasian crane (*Grus grus*) feathers $\delta^{18}\text{O}$ values and modelled $\delta^{18}\text{O}$ of ambient water at the feather collection sites. Water isotope estimates are (a) global-fixed regression–interpolation-based precipitation $\delta^{18}\text{O}$ isoscape (Bowen & Revenaugh, 2003), (b) regionalized cluster-based precipitation isoscape (Terzer *et al.*, 2013), (c) GCM-based precipitation $\delta^{18}\text{O}$ and (d) GCM-based soil water $\delta^{18}\text{O}$ isoscapes (Haese *et al.*, 2013). The values are mean \pm SD for two replicates for every vane subsample.

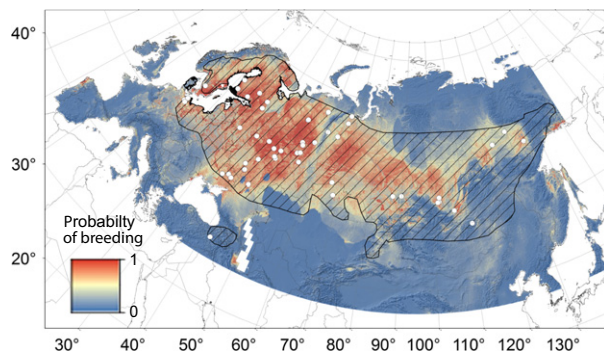


Figure 3 Probability surface of the Eurasian crane (*Grus grus*) potential breeding areas as estimated by MAXENT model (current study) and occurrence points used for the model (shown on the map as grey circles). The elevation is represented by the topography of the map. The diagonal striped area indicates a previously reported breeding range (Johnsgard, 1983). The cell size was 1×1 km. Projection: Albers.

the upper 33% of the cumulative density functions, for assignment based on the two isotopes. This is illustrated for two birds assigned to the rescaled isoscapes: sample 39 ($\delta^{18}\text{O}_f = 14.0\text{‰}$, $\delta^2\text{H}_f = -60.7\text{‰}$) was assigned to eastern Europe and part of southern Russia (Fig. 4a,b), while sample 28 ($\delta^{18}\text{O}_f = 6.7\text{‰}$, $\delta^2\text{H}_f = -121.6\text{‰}$) was assigned to more eastern portion of the known breeding range for cranes (Fig. 4c,d).

We assigned all 102 samples to the $\delta^{18}\text{O}_f$ and $\delta^2\text{H}_f$ rescaled isoscapes and summed the resulting posterior probabilities of origin (without reclassification) to establish the origin at the population level (Fig. 5). Both the $\delta^{18}\text{O}$ and $\delta^2\text{H}$ data suggest that most individuals likely originate from the area around the Baltic Sea and east Europe, whereas a smaller proportion of individuals are from western Russia

(Fig. 5). A small proportion of individuals originated from the western area of the Asian portion of the breeding range (Fig. 5), while for two of these individuals (e.g. Fig. 4c,d), most of the assigned area (>90% for $\delta^{18}\text{O}$ and >60% for $\delta^2\text{H}$) fell rather far east of the Ural Mountains.

DISCUSSION

This study demonstrates the ability of $\delta^{18}\text{O}$ feather measurements to reveal the origins of migratory birds at a broad spatial scale. Our results indicate that the use of the soil water isoscape was a more appropriate choice for $\delta^{18}\text{O}$, while the precipitation isoscape performed better for $\delta^2\text{H}$. Additionally, the use of the MAXENT model to generate a probabilistic distribution map as a Bayesian prior for assignment allowed the elimination of areas unlikely to represent species' origin. The tools implemented in this study may significantly improve our capacity to quantify migratory connectivity of species inhabiting poorly studied areas and hence are important for conservation efforts of many migratory bird species. However, to further test the application of these approaches, comparisons of model outputs against isotopic measurements from a large and spatially explicit sample of individuals from known origin are clearly required.

While a latitudinal $\delta^2\text{H}_f$ pattern has been well established for North America and Europe (Bowen *et al.*, 2005; Norris *et al.*, 2006; Sellick *et al.*, 2009), this study is the first to examine and show a longitudinal $\delta^{18}\text{O}_f$ and $\delta^2\text{H}_f$ pattern for Asia. This longitudinal pattern matches data from the four largest arctic rivers and 13 monitoring stations across Russia, implying that eastward cross-continental moisture transport generates more depleted precipitation further inland (Kurita, 2004; Yi *et al.*, 2012). This longitudinal gradient is also presented in the RCWIP-based and GCM-based isoscapes but less evident in the traditionally used GFRI-based isoscape (Table 2),

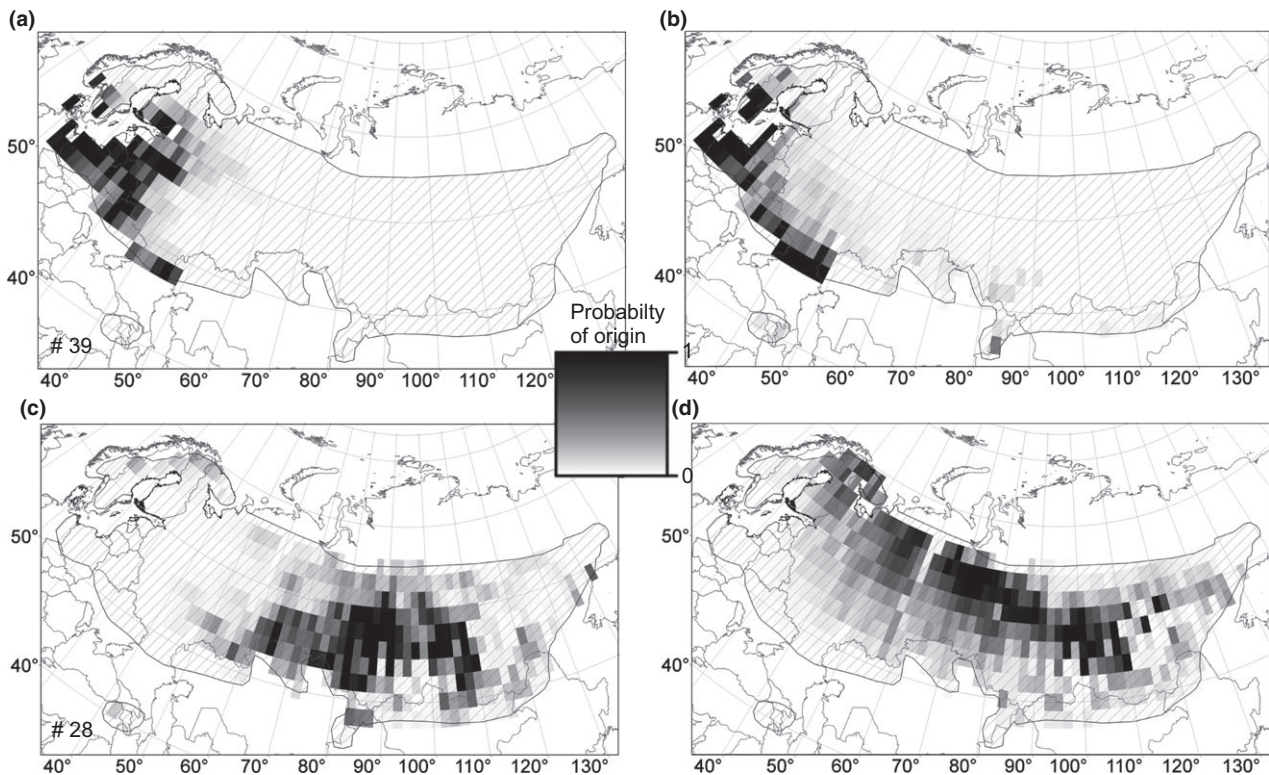


Figure 4 Predicted probability surfaces of origin for two individuals sampled in the Hula Valley (sample 39, $\delta^{18}\text{O}_f = 14.0\text{‰}$ and $\delta^2\text{H}_f = -60.7$ and sample 28, $\delta^{18}\text{O}_f = 6.7\text{‰}$ and $\delta^2\text{H}_f = -121.6$) for which the congruence between the upper 33% of the cumulative density function for assignment based on $\delta^{18}\text{O}$ and $\delta^2\text{H}$ data was 31% and 24%, respectively. Panels (a) and (c) show assignment performed on the GCM-based soil water $\delta^{18}\text{O}$ ($\delta^{18}\text{O}_{\text{GCM-s}}$) isoscape (Haese *et al.*, 2013). Panels (b) and (d) show assignment performed on the RCWIP-based precipitation $\delta^2\text{H}$ ($\delta^2\text{H}_{\text{RCWIP-p}}$) isoscape (Terzer *et al.*, 2013). The panels show posterior probabilities of origin without reclassification. The cell size was 0.18 degrees. Projection: Albers.

indicating that, in agreement with Terzer *et al.* (2013), for areas with low isotopic data coverage, the RCWIP-based isoscape is preferable to the GFRI-based isoscape.

The only published assessment of the $\delta^{18}\text{O}_f$ – $\delta^{18}\text{O}_p$ relationship (Hobson *et al.*, 2004) was based on the GFRI-based isoscape but performed in Europe where the coverage of measurement stations is good. The $\delta^{18}\text{O}_f$ – $\delta^{18}\text{O}_p$ correlation reported in that study ($r^2 = 0.57$) is similar to the correlation we found with the GCM-based $\delta^{18}\text{O}_p$ and $\delta^{18}\text{O}_{\text{RCWIP-p}}$ values ($r^2 = 0.59$ and $r^2 = 0.61$, respectively) despite the difference in the sample size. The stronger $\delta^{18}\text{O}_f$ – $\delta^{18}\text{O}_{\text{GCM-s}}$ correlation ($r^2 = 0.78$) may be caused by the soil water isotopic signal being a more time-integrated signal of hydrological processes occurring on land surfaces, while the precipitation signal rather reflects atmospheric conditions, varying on shorter time-scales [a detailed description of the hydrological processes incorporated into ECHAM5-JSBACH-wiso can be found in Haese *et al.* (2013)]. However, we again recognize the need for much further ground-truthing of this approach which would require direct comparisons between modelled outputs and actual measurements of precipitation, soil moisture and higher trophic-level consumers.

Strong correlation found in human hair (Bowen *et al.*, 2009), dragonfly wings (Hobson *et al.*, 2012) and several

farm animals (Chesson *et al.*, 2011) between tissue $\delta^{18}\text{O}$ and $\delta^2\text{H}$ values, reflecting the basal meteoric core relationship, was not found in this study. This difference might be explained by these organisms being well-hydrated compared to cranes, as higher water volume processed by the body leads to more similar values of body water and drinking water $\delta^{18}\text{O}$ and $\delta^2\text{H}$ (O'Grady *et al.*, 2010). In contrast, feline carnivores showed no correlation between hair and water $\delta^{18}\text{O}$ (Pietsch *et al.*, 2011). This may suggest that the decoupling found between the $\delta^{18}\text{O}_f$ and $\delta^2\text{H}_f$ in this study may be influenced by the relative role of hydration in the overall nutrition of cranes.

The use of the MAXENT model allows estimating probabilities of suitable breeding areas throughout the crane breeding range, thus enabling incorporation of prior information into the assignment. For example, high-elevation regions in the Asian portion of the known breeding range are unsuitable for cranes (Johnsgard, 1983) and are thus unlikely to be their origin (Figs 3 & 4). In most of the predicted distribution areas which fell outside of the known breeding range (assumed to be the most updated approximation of the cranes' realized breeding niche) (Fig. 3), the species was reported in the past as a common breeder but disappeared as a breeder over the last 200–400 years (Johnsgard, 1983).

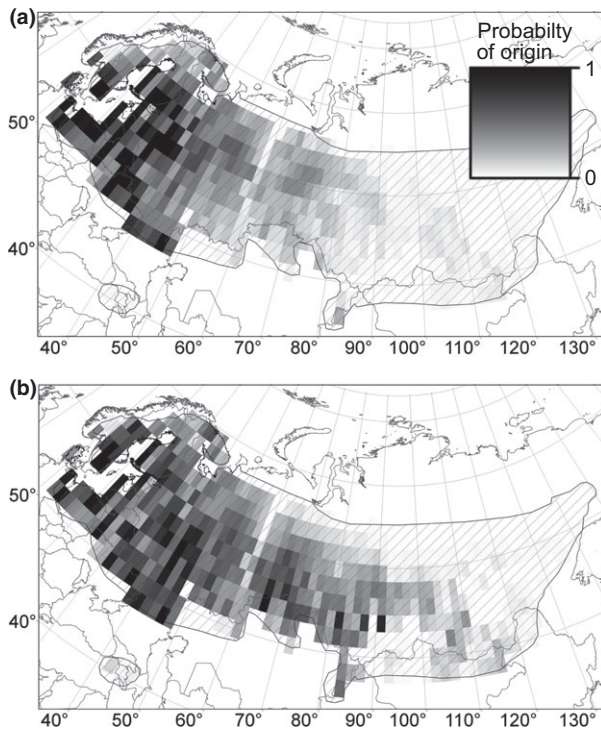


Figure 5 Predicted posterior probabilities of origin, based on the application of the Bayesian Rule incorporating prior probabilities depicted in Fig. 3, normalized to maximum value found over all cells for all the Eurasian crane (*Grus grus*) individuals sampled in the Hula Valley. Panel (a) shows assignment performed on the GCM-based soil water $\delta^{18}\text{O}$ ($\delta^{18}\text{O}_{\text{GCM-s}}$) isoscape (Haese *et al.*, 2013). Panel (b) shows assignment performed on the RCWIP-based precipitation $\delta^2\text{H}$ ($\delta^2\text{H}_{\text{RCWIP-p}}$) isoscape (Terzer *et al.*, 2013). The cell size was 0.18 degrees. Projection: Albers.

However, niche-based models provide an approximation of the potential niche on the basis of climatic and habitat variables associated with the species occurrence locations, and do not account for a reduction of the realized niche as a consequence of, for instance, habitat loss and other anthropogenic disturbances. Consequently, the predicted areas should be treated with some caution. Thus, in cases when additional information is available (e.g. breeding pair count data, disturbance level), it can be incorporated to improve model predictions.

Over a broad scale, and at the spatial resolution permitted by this method, the cranes wintering in and migrating through the Hula Valley arrived from a wide range of areas throughout the known breeding range of the species (Fig. 5). Despite the decoupling found between the $\delta^{18}\text{O}_f$ and $\delta^2\text{H}_f$, assignment based on both isotopes similarly showed that >85% of the cranes sampled in the Hula Valley were assigned to the area west of the Ural Mountains, while for two individuals, most of the assigned area was farther east. These findings must be treated with caution, but may suggest that some of the cranes breeding east of the Ural Mountains may migrate to and through the Middle East. These cranes may use the Black Sea–Mediterranean or the East African–West

Asian flyways, both of which include bird species that breed in regions of West Siberia and migrate through the Middle East and Israel in particular. These flyways are well known for many waterfowl species (Stroud *et al.*, 2004) but were not previously shown to be used by cranes. However, since only a low proportion of individuals were assigned to these regions, an alternative explanation to this phenomenon may be that they had accidentally drifted from their principal migration routes and joined other, west-originated flocks migrating to the Middle East. Since such vagrant individuals also face the longest journey compared to the other individuals migrating to the Hula Valley, there might be a bias on the estimate of the proportion of this population as a consequence of our sampling of carcasses, and thus, a more systematic sampling may be required to identify better the contribution of different breeding areas to the population in the Hula Valley.

CONCLUSIONS AND FUTURE APPLICATIONS

We suggest further testing and application of the approaches we introduced in the current study for enriching the toolbox for species and sites for which stable isotope application was previously limited. Further investigation of the processes that influence the link between tissue $\delta^{18}\text{O}$ and that of surface water, ground water and precipitation may shed light on the reasons for the strong $\delta^{18}\text{O}_f$ – $\delta^{18}\text{O}_{\text{GCM-s}}$ correlation we found. We thus call for establishment of rescaling algorithms linking $\delta^{18}\text{O}_f$ values with ambient water values based on bird species from known moult origins, similar to those already established at continental scales for $\delta^2\text{H}_f$ (Hobson *et al.*, 2012). Moreover, we encourage using multiple tracers to improve model predictions as it was previously shown to increase the resolution of assignment tests (Chamberlain *et al.*, 1997; Hobson, 1999).

To explain the decoupling found between tissue $\delta^{18}\text{O}$ and $\delta^2\text{H}$ of some organisms but not others, further investigations of factors determining isotope fractionation during metabolic and tissue formation processes are needed. Significant modelling and empirical research remains to be performed to elucidate taxa-specific and physiological factors which govern the integration of ambient water $\delta^{18}\text{O}$ and $\delta^2\text{H}$ into animal proteins.

We also propose the use of the MAXENT model as a general framework for estimating the breeding distribution of (the many) inadequately mapped species. The main advantage of this approach is in not being ‘data hungry’: the MAXENT model requires relatively small amounts of occurrence data which are readily available for many (perhaps most) species around the world from surveys, researchers or the free GBIF database (<http://data.gbif.org>), as demonstrated here for cranes. Because MAXENT is a probabilistic tool, it can be readily used in current Bayesian isotopic assignment models as a prior to better constrain potential origins. This will require proper consideration of how errors propagate throughout the experimental and modelling process to determine uncertainty in the predicted assignments.

ACKNOWLEDGEMENTS

The authors thank A. Artemyev, A. Menshikov, E. Ilyashenko, G. Nowald, I. Fefelov, J. Leppänen, K. Michail, M. Korepov, N. Donner, N. Günter, P. Mustakallio, P. Raukko, S. Lundgren, S. Winter, T. Kashenseva, V. Degtyaryev, V. Degtyaryev and Y. Markin for sample collection at the breeding areas. We are grateful to Agmon Hula, Agalili safari wagon staff, E. Galili, Y. Davidson and O. Hatzofe for their help in Hula Valley sample collection. We thank the members of Nathan's Movement Ecology and Angert's Laboratories, especially Y. Bartan and S. Mazeh for their help during the research. This research was supported by a GIF grant I-999-66.8/2008 to RN and an operating grant to KAH from Environment Canada. RN also acknowledges support from the Adelina and Massimo Della Pergola Chair of Life Sciences, and the Minerva Center for Movement Ecology. We also thank three anonymous referees for their useful comments on an earlier draft of this manuscript.

REFERENCES

- Amante, C. & Eakins, B.W. (2009) *ETOPO1 1 arc-minute global relief model: procedures, data sources and analysis*. NOAA Technical Memorandum NESDIS NGDC-24, Boulder, CO, pp. 19.
- Boulet, M. & Norris, D.R. (2006) The past and present of migratory connectivity. *Ornithological Monographs*, **61**, 1–13.
- Bowen, G.J. & Revenaugh, J. (2003) Interpolating the isotopic composition of modern meteoric precipitation. *Water Resources Research*, **39**, 1–13.
- Bowen, G.J., Wassenaar, L.I. & Hobson, K.A. (2005) Global application of stable hydrogen and oxygen isotopes to wildlife forensics. *Oecologia*, **143**, 337–348.
- Bowen, G.J., Ehleringer, J.R., Chesson, L.A., Thompson, A.H., Podlesak, D.W. & Cerling, T.E. (2009) Dietary and physiological controls on the hydrogen and oxygen isotope ratios of hair from mid-20th century indigenous populations. *American Journal of Physical Anthropology*, **139**, 494–504.
- Bryant, J.D. & Froelich, P. (1995) A model of oxygen isotope fractionation in body water of large mammals. *Geochimica et Cosmochimica Acta*, **59**, 4523–4537.
- Chamberlain, C.P., Blum, J.D., Holmes, R.T., Feng, X., Sherry, T.W. & Graves, G.R. (1997) The use of isotope tracers for identifying populations of migratory birds. *Oecologia*, **109**, 132–141.
- Chesson, L.A., Valenzuela, L.O., Bowen, G.J., Cerling, T.E. & Ehleringer, J.R. (2011) Consistent predictable patterns in the hydrogen and oxygen stable isotope ratios of animal proteins consumed by modern humans in the USA. *Rapid Communications in Mass Spectrometry*, **25**, 3713–3722.
- Craig, H. (1961) Standards for reporting concentrations of deuterium and oxygen-18 in natural waters. *Science*, **133**, 1833–1834.
- Dansgaard, W. (1964) Stable isotopes in precipitation. *Tellus*, **16**, 436–468.
- Dormann, C.F., Elith, J., Bacher, S., Buchmann, C., Carl, G., Carré, G., Marquéz, J.R.G., Gruber, B., Lafourcade, B., Leitão, P.J., Münkemüller, T., McClean, C., Osborne, P.E., Reineking, B., Schröder, B., Skidmore, A.K., Zurell, D. & Lautenbach, S. (2013) Collinearity: a review of methods to deal with it and a simulation study evaluating their performance. *Ecography*, **36**, 027–046.
- Elith, J., Graham, C.H., Anderson, R.P. *et al.* (2006) Novel methods improve prediction of species' distributions from occurrence data. *Ecography*, **29**, 129–151.
- Haese, B., Werner, M. & Lohmann, G. (2013) Stable water isotopes in the coupled atmosphere–land surface model ECHAM5-JSBACH. *Geoscientific Model Development*, **6**, 1463–1480.
- Hijmans, R.J., Cameron, S.E., Parra, J.L., Jones, P.G. & Jarvis, A. (2005) Very high resolution interpolated climate surfaces for global land areas. *International Journal of Climatology*, **25**, 1965–1978.
- Hobson, K.A. (1999) Tracing origins and migration of wildlife using stable isotopes: a review. *Oecologia*, **120**, 314–326.
- Hobson, K.A. (2005) Stable isotopes and the determination of avian migratory connectivity and seasonal interactions. *The Auk*, **122**, 1037.
- Hobson, K.A. (2011) Isotopic ornithology: a perspective. *Journal of Ornithology*, **152**, 49–66.
- Hobson, K. & Wassenaar, L. (2008) *Tracking animal migration with stable isotopes*, 2nd edn. Academic Press, London.
- Hobson, K.A., Bowen, G.J., Wassenaar, L.I., Ferrand, Y. & Lormee, H. (2004) Using stable hydrogen and oxygen isotope measurements of feathers to infer geographical origins of migrating European birds. *Oecologia*, **141**, 477–488.
- Hobson, K.A., Soto, D.X., Paulson, D.R., Wassenaar, L.I. & Matthews, J.H. (2012) A dragonfly ($\delta^2\text{H}$) isoscape for North America: a new tool for determining natal origins of migratory aquatic emergent insects. *Methods in Ecology and Evolution*, **3**, 766–772.
- Hoffmann, G., Werner, M. & Heimann, M. (1998) Water isotope module of the ECHAM atmospheric general circulation model: a study on timescales from days to several years. *Journal of Geophysical Research*, **103**, 16871.
- Johnsgard, P. (1983) *Cranes of the world*. Indiana University Press, Bloomington.
- Jouzel, J., Russell, G.L., Suozzo, R.J., Koster, R.D., White, J.W.C. & Broecker, W.S. (1987) Simulations of the HDO and H_2^{18}O atmospheric cycles using the NASA GISS general circulation model: the seasonal cycle for present-day conditions. *Journal of Geophysical Research*, **92**, 14739.
- Kashentseva, T.A. (2003) ЛИНЬКА СЕРОГО ЖУРАВЛЯ (*Grus grus*) В УСЛОВИЯХ НЕВОЛИ. *Сборник трудов Окского заповедника*, 281–302.
- Kramer-Schadt, S., Niedballa, J., Pilgrim, J.D. *et al.* (2013) The importance of correcting for sampling bias in MaxEnt species distribution models. *Diversity and Distributions*, **19**, 1366–1379.
- Kurita, N. (2004) Modern isotope climatology of Russia: a first assessment. *Journal of Geophysical Research*, **109**, D03102.

- Lehner, B. & Döll, P. (2004) Development and validation of a global database of lakes, reservoirs and wetlands. *Journal of Hydrology*, **296**, 1–22.
- Martin, T.G., Chadès, I., Arcese, P., Marra, P.P., Possingham, H.P. & Norris, D.R. (2007) Optimal conservation of migratory species. *PLoS ONE*, **2**, e751.
- Meier-Augenstein, W., Hobson, K.A. & Wassenaar, L.I. (2013) Critique: measuring hydrogen stable isotope abundance of proteins to infer origins of wildlife, food and people. *Bioanalysis*, **5**, 751–767.
- Norris, D.R., Marra, P.P., Bowen, G.J., Ratcliffe, L.M., Royle, J.A. & Kyser, T.K. (2006) Migratory connectivity of a widely distributed songbird, the American Redstart (*Setophaga ruticilla*). *Ornithological Monographs*, **61**, 14–28.
- O’Grady, S.P., Wende, A.R., Remien, C.H., Valenzuela, L.O., Enright, L.E., Chesson, L.a., Abel, E.D., Cerling, T.E., & Ehleringer, J.R. (2010) Aberrant water homeostasis detected by stable isotope analysis. *PLoS ONE*, **5**, e11699.
- Phillips, S.J., Anderson, R.P. & Schapire, R.E. (2006) Maximum entropy modeling of species geographic distributions. *Ecological Modelling*, **190**, 231–259.
- Pietsch, S.J., Hobson, K.A., Wassenaar, L.I. & Tütken, T. (2011) Tracking cats: problems with placing feline carnivores on δO , δD isoscapes. *PLoS ONE*, **6**, e24601.
- Qi, H., Coplen, T.B. & Wassenaar, L.I. (2011) Improved online $\delta^{18}\text{O}$ measurements of nitrogen- and sulfur-bearing organic materials and a proposed analytical protocol. *Rapid Communications in Mass Spectrometry: RCM*, **25**, 2049–2058.
- Rolshausen, G., Segelbacher, G., Hobson, K.A. & Schaefer, H.M. (2009) Contemporary evolution of reproductive isolation and phenotypic divergence in sympatry along a migratory divide. *Current Biology*, **19**, 2097–2101.
- Rubenstein, D.R. & Hobson, K.A. (2004) From birds to butterflies: animal movement patterns and stable isotopes. *Trends in Ecology & Evolution*, **19**, 256–263.
- Sellick, M.J., Kyser, T.K., Wunder, M.B., Chipley, D. & Norris, D.R. (2009) Geographic variation of strontium and hydrogen isotopes in avian tissue: implications for tracking migration and dispersal. *PLoS ONE*, **4**, e4735.
- Shanni, I., Labinger, Z., Nathan, R. & Alon, D. (2011) *Crane energetics and management technique – final report*. KKL and USFS Program, Tel Aviv, Isreal, pp 39.
- Shirihai, H. (1996) *The birds of Israel*. Academic press, London.
- St Amour, N.A., Gibson, J.J., Edwards, T.W.D., Prowse, T.D. & Pietroniro, A. (2005) Isotopic time-series partitioning of streamflow components in wetland-dominated catchments, lower Liard River basin, Northwest Territories, Canada. *Hydrological Processes*, **19**, 3357–3381.
- Stroud, D.A., Davidson, N.C., West, R., Scott, D.A., Haanstra, L., Thorup, O., Ganter, B. & Delany, S. (compilers) on behalf of the International Wader Study Group (2004) Status of migratory wader populations in Africa and Western Eurasia in the 1990s. *International Wader Studies*, **15**, 1–259.
- Terzer, S., Wassenaar, L.I., Araguás-Araguás, L.J. & Aggarwal, P.K. (2013) Global isoscapes for $\delta^{18}\text{O}$ and $\delta^2\text{H}$ in precipitation: improved prediction using regionalized climatic regression models. *Hydrology and Earth System Sciences*, **17**, 4713–4728.
- Wassenaar, L.I. & Hobson, K.A. (2003) Comparative equilibration and online technique for determination of non-exchangeable hydrogen of keratins for use in animal migration studies. *Isotopes in Environmental and Health Studies*, **39**, 211–217.
- Wassenaar, L.I. & Hobson, K.A. (2006) Stable-hydrogen isotope heterogeneity in keratinous materials : mass spectrometry and migratory wildlife tissue subsampling strategies. *Rapid Communications in Mass Spectrometry*, **20**, 2505–2510.
- Webster, M. & Marra, P.P. (2005) The importance of understanding migratory connectivity and seasonal interactions. *Birds of two worlds: the ecology and evolution of migration* (ed. by P.P. Marra and R. Greenberg), pp. 197–209. JHU Press, Baltimore.
- Webster, M.S., Marra, P.P., Haig, S.M., Bensch, S. & Holmes, R.T. (2002) Links between worlds: unraveling migratory connectivity. *Trends in Ecology & Evolution*, **17**, 76–83.
- Werner, M., Langebroek, P.M., Carlsen, T., Herold, M. & Lohmann, G. (2011) Stable water isotopes in the ECHAM5 general circulation model: toward high-resolution isotope modeling on a global scale. *Journal of Geophysical Research*, **116**, D15109.
- Wunder, M.B. (2010) Using Isoscapes to Model Probability Surfaces for Determining Geographic Origins. *Isoscapes* (ed. by J.B. West, G.J. Bowen, T.E. Dawson and K.P. Tu), pp. 251–270. Springer, Dordrecht, Netherlands.
- Yi, Y., Gibson, J.J., Cooper, L.W., Hélie, J.-F., Birks, S.J., McClelland, J.W., Holmes, R.M. & Peterson, B.J. (2012) Isotopic signals (^{18}O , ^2H , ^3H) of six major rivers draining the pan-Arctic watershed. *Global Biogeochemical Cycles*, **26**, GB1027.

SUPPORTING INFORMATION

Additional Supporting Information may be found in the online version of this article:

Appendix S1 Sample cleaning and preparation for stable oxygen isotope analysis.

Table S1 Collection site coordinates and $\delta^{18}\text{O}$ values for samples collected at the breeding sites.

Table S2 Collection date and $\delta^{18}\text{O}$ values for samples collected in the Hula Valley during the non-breeding period.

Table S3 Summary of the breeding locations described in the literature and the annual reports of the “Crane working group of Eurasia”.

Table S4 Occurrence data used for creation of the probabilistic breeding distribution map.

Table S5 Global legend for the land cover map, with its vegetation classes.

Table S6 Global Climatic variables.

BIOSKETCH

Sasha Pekarsky is an ecologist who has completed her MSc studies on migration of Eurasian cranes at the Hebrew University in Jerusalem (Jerusalem, Israel) under the supervision of R.N. and A.A. She is interested in movement ecology,

bird migration and conservation. B.H. and M.W developed the isotope-enabled general circulation model. K.A.H. provided advice on stable isotope methods and data analysis.

Editor: David M. Richardson